

## Supplementary Information

### Lead isotopes in deep sea sediments reveal alteration of the isotopic composition signal in the water column at highly productive sites in the South Atlantic Ocean

Lina Oskamp, Marta Pérez Rodríguez, Adelina Calean, Olaf Rienitz, Klaus-Holger Knorr, Kazumasa Oguri, Masashi Tsuchiya, Marco Benkhettab Sindlev, Stephan Krisch, Arianna Olivelli, Frank Wenzhöfer, Ronnie N. Glud, Harald Biester

#### Table of contents

##### Figures

Figure S1 Composite picture showing sediment cores from St9, St15 and St16.

Figure S2 Boxplots displaying organic constituents and Al concentrations.

Figure S3 Boxplots displaying (trace) element concentrations.

Figure S4 Boxplots displaying Pb isotope ratios.

Figure S5 Depth profiles of the  $^{206}\text{Pb}/^{207}\text{Pb}$  ratios, Fe, Mn, Ca, P, Ba and TC at St15.

Figure S6 Depth profiles of the  $^{206}\text{Pb}/^{207}\text{Pb}$  ratios, Fe, Mn, Ca, P, Ba and TC at St16.

Figure S7 Depth profiles of the  $^{206}\text{Pb}/^{207}\text{Pb}$  ratios, Fe, Mn, Ca, P, Ba and TC at St9.

Figure S8 Pb concentrations plotted against Ba concentrations ( $\mu\text{g g}^{-1}$ ).

Figure S9 Pb concentrations plotted against Al concentrations ( $\mu\text{g g}^{-1}$ ).

Figure S10 Pb/Al ratios plotted against Pb/P ratios at all stations.

Figure S11 Profiles of  $^{210}\text{Pb}_{\text{ex}}$  concentrations from St9, St15 and St16.

Figure S12 Average Pb/TOC-ratios at St9, 15 and 16 plotted against the station water depth.

Figure S13 Correlation matrix for the sediments at St15.

Figure S14 Correlation matrix for the sediments at St16.

Figure S15 Correlation matrix for the sediments at St9.

##### Tables

Table S1 Key characteristics of St9, 15 and 16.

Table S2 Correlation coefficients of Pb isotope ratios and selected sediment constituents.

## **Methods**

### **Detailed description of the determination of Pb isotopes**

#### **Sample preparation**

Table S3: Pb separation sequence according to the slightly modified Eichrom application report OTS01.

#### **Pb isotope measurements**

Table S4: Cup configuration used for all measurements.

Table S5: MC-ICP-MS parameters applied for the measurements.

### **Detailed description of the analysis of trace elements**

Table S6: Certified values for reference material IAEA 456 ( $n = 12$ ) and measured average concentrations and standard deviations (SD) of the digested material.

### **CNS analysis**

Table S7: Certified TOC contents for reference materials and measured average concentrations and standard deviations (SD).

### **<sup>210</sup>Pb Dating**

Table S8: Depth, Cumulative mass, and <sup>210</sup>Pb<sub>ex</sub> concentrations of St9, St15, and S516 cores.

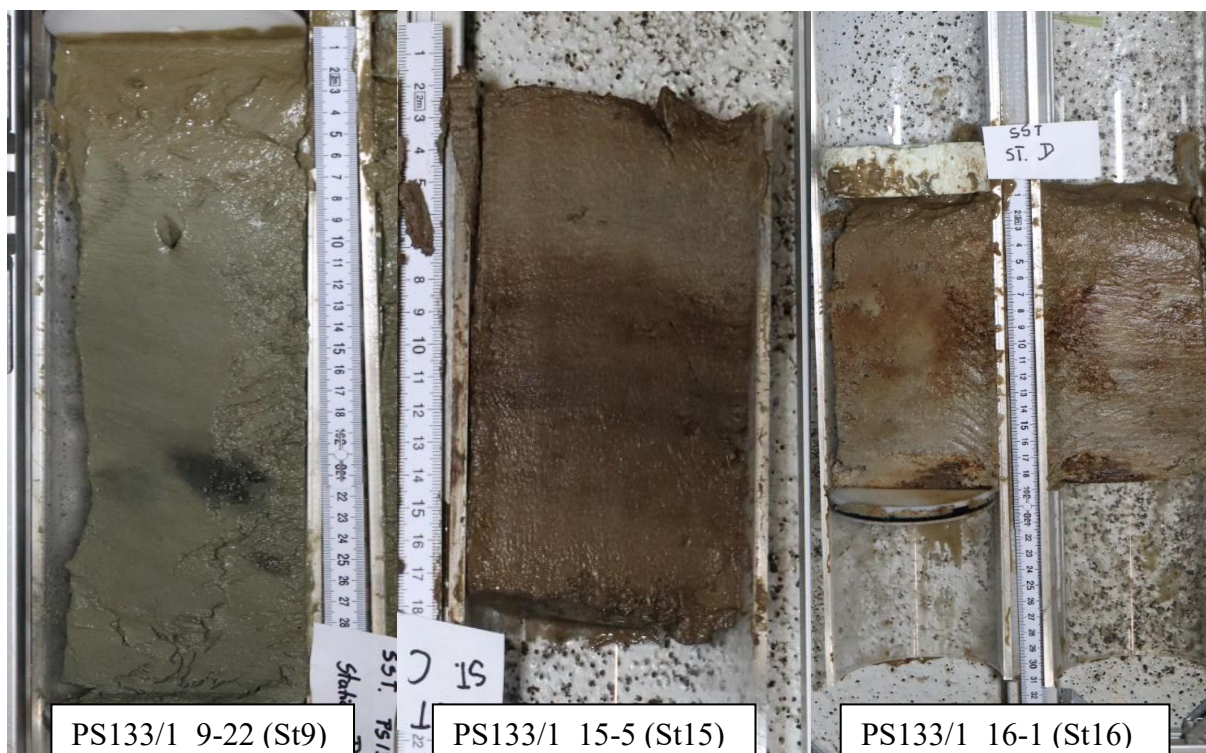


**Figure S1:** Composite picture showing sediment cores from St9, St15 and St16 (from left to right) directly after sampling. 0 cm depth is positioned at the top for each core. Pictures were taken and provided by Ronnie N. Glud.

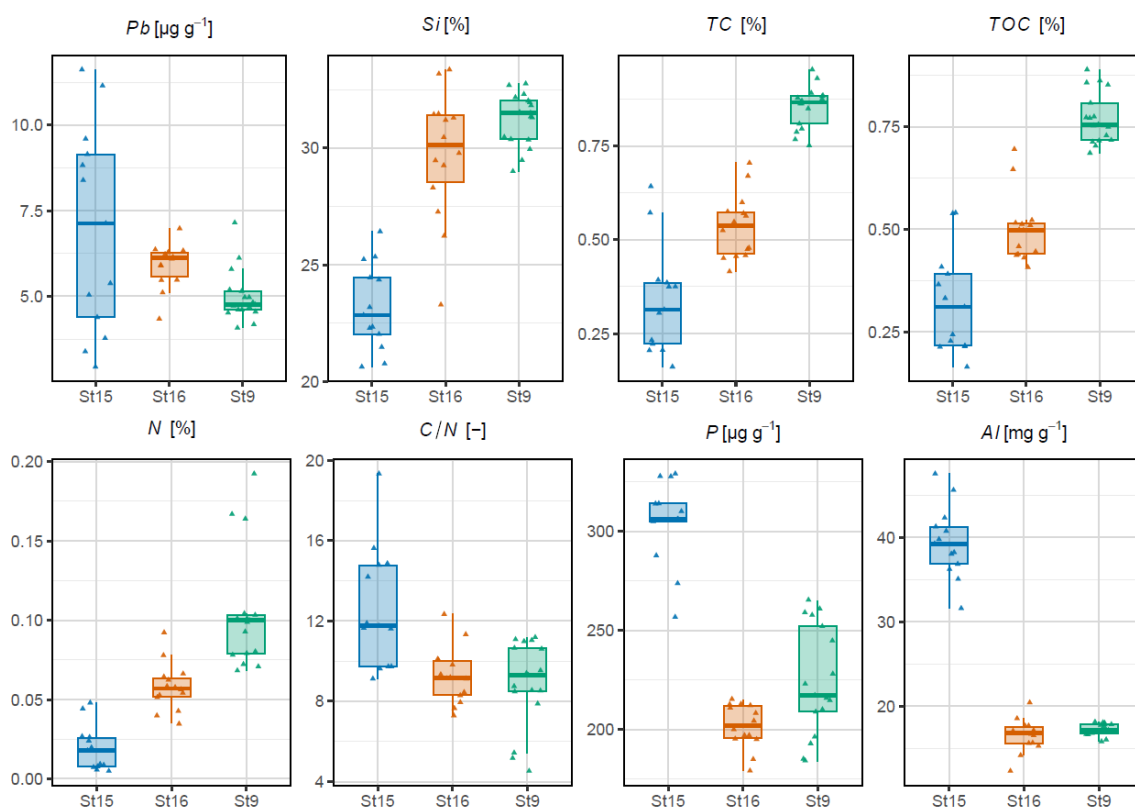


**Figure S2:** Boxplots displaying organic constituents and Al concentrations (% / $\mu\text{g g}^{-1}$  / $\text{mg g}^{-1}$ ) in the cores from St9, St15 and St16. Provided are upper and lower quartiles, median, outliers (centered above/below the plot) and original data points (scattered in the plot range).

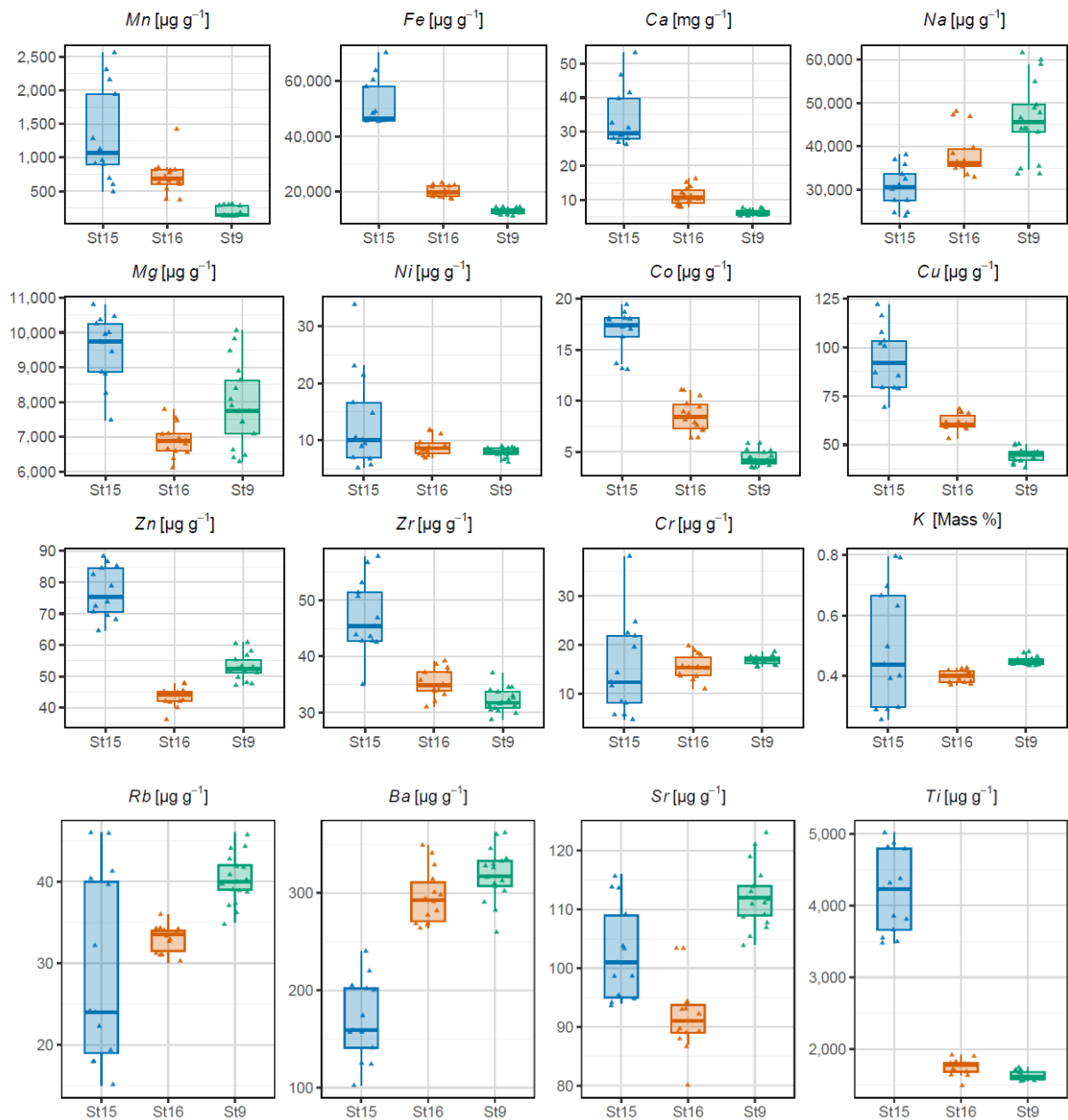


**Figure S3:** Boxplots displaying (trace) element concentrations ( $\mu\text{g g}^{-1}$  /  $\text{mg g}^{-1}$ ) in the cores from St9, St15 and St16. Provided are upper and lower quartiles, median, outliers (centered above/below the plot) and original data points (scattered in the plot range).

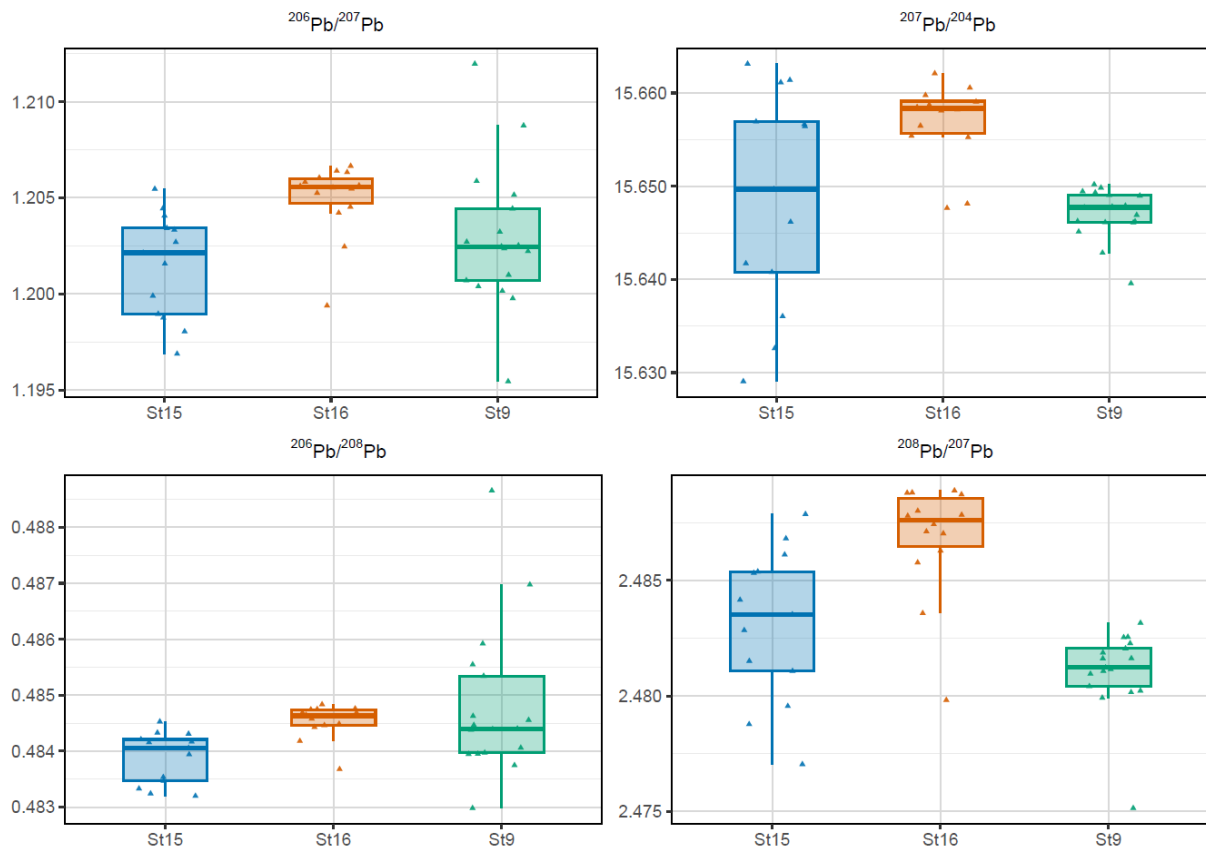


**Figure S4:** Boxplots displaying Pb isotope ratios in sediment cores from St9, St15 and St16. Provided are upper and lower quartiles, median, outliers (centered above/below the plot) and original data points (scattered in the plot range).

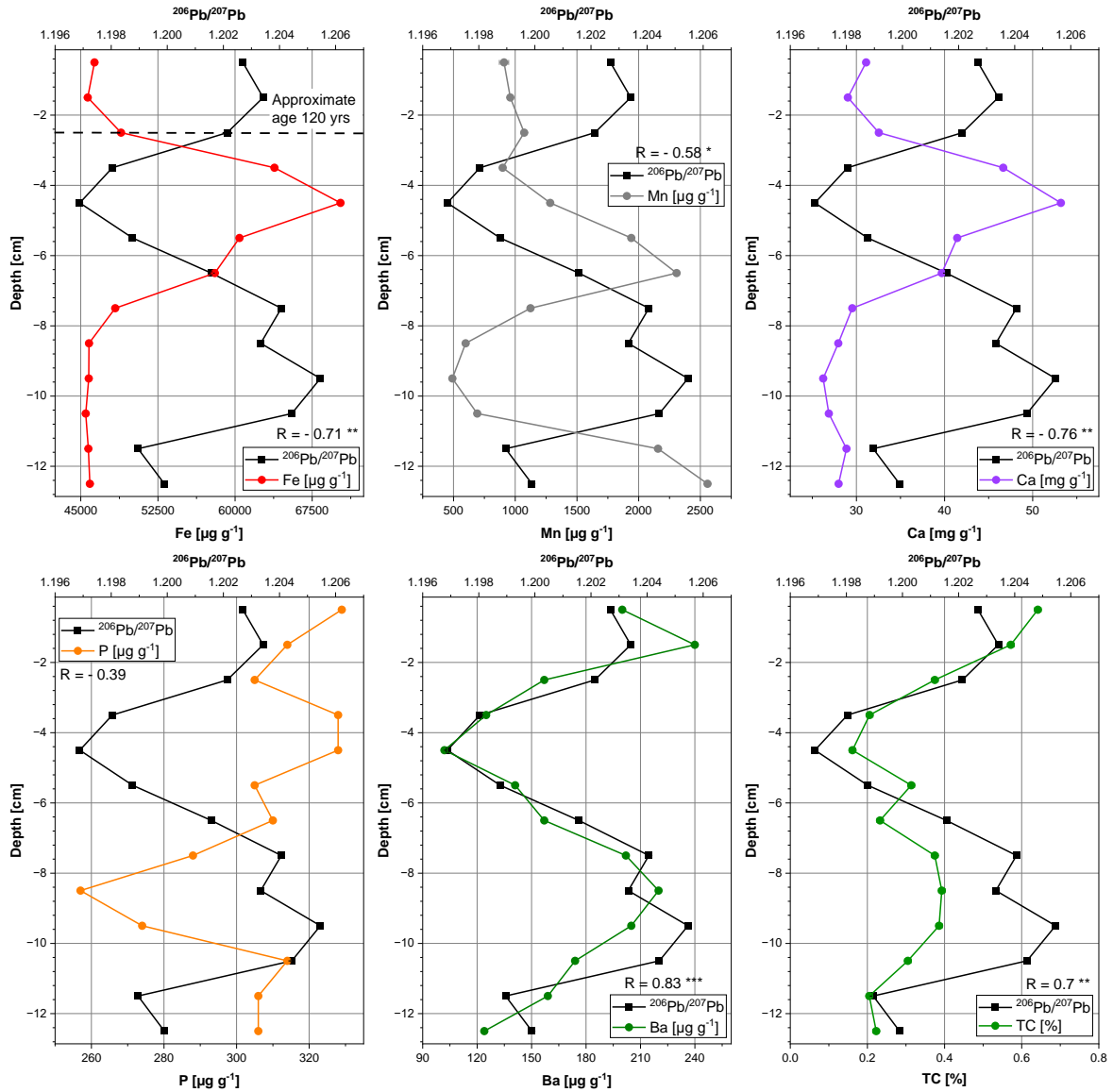


**Figure S5:** Depth profiles of the  $^{206}\text{Pb}/^{207}\text{Pb}$  ratios, Fe, Mn, Ca, P, Ba and TC concentrations ( $\%$  /  $\mu\text{g g}^{-1}$  /  $\text{mg g}^{-1}$ ) in the sediment core from St15. Error bars are included but, in some cases, smaller than the symbols.

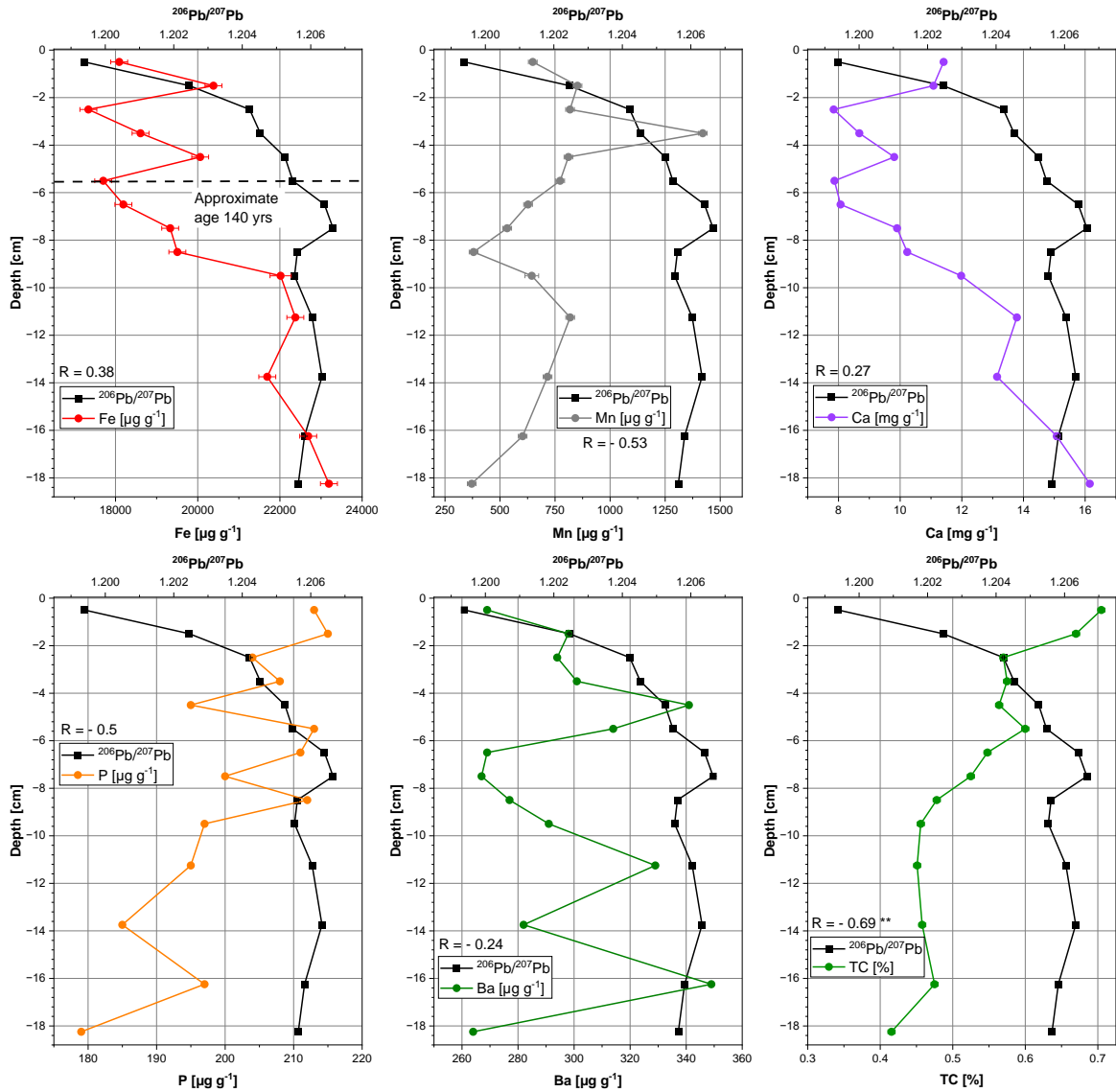


**Figure S6:** Depth profiles of the  $^{206}\text{Pb}/^{207}\text{Pb}$  ratios, Fe, Mn, Ca, P, Ba and TC concentrations ( $\%$  /  $\mu\text{g g}^{-1}$  /  $\text{mg g}^{-1}$ ) in the sediment core from St16. Error bars are included but, in some cases, smaller than the symbols.

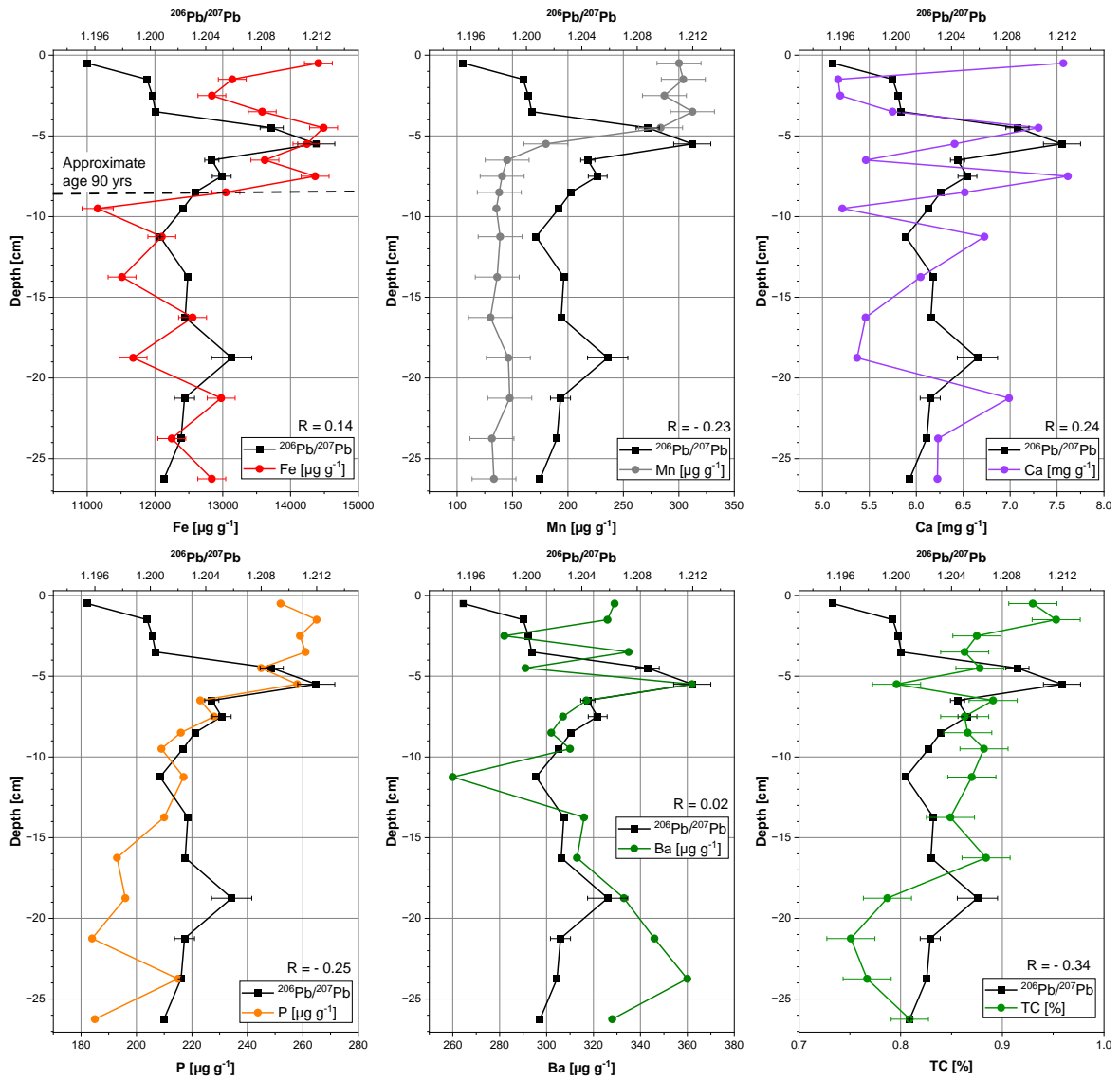


**Figure S7:** Depth profiles of the  $^{206}\text{Pb}/^{207}\text{Pb}$  ratios, Fe, Mn, Ca, P, Ba and TC concentrations ( $\%$  /  $\mu\text{g g}^{-1}$  /  $\text{mg g}^{-1}$ ) in the sediment core from St9. Error bars are included but, in some cases, smaller than the symbols.

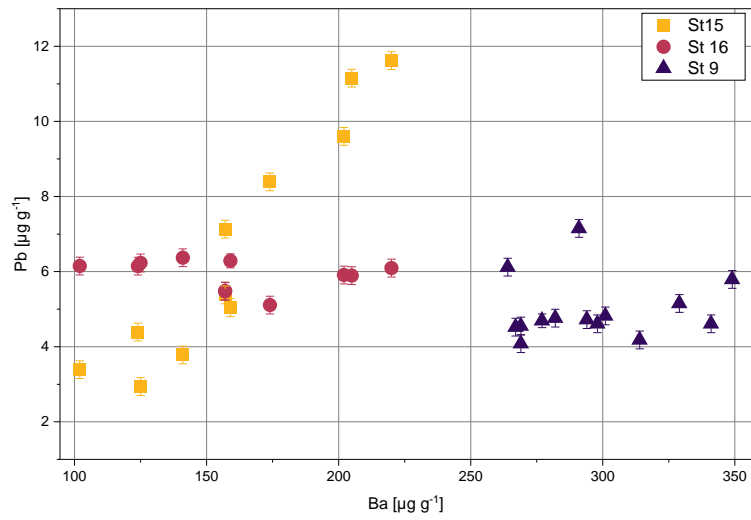


**Figure S8:** Pb concentrations plotted against Ba concentrations ( $\mu\text{g g}^{-1}$ ) at all stations. Error bars are included, but are in some cases smaller than the symbols.

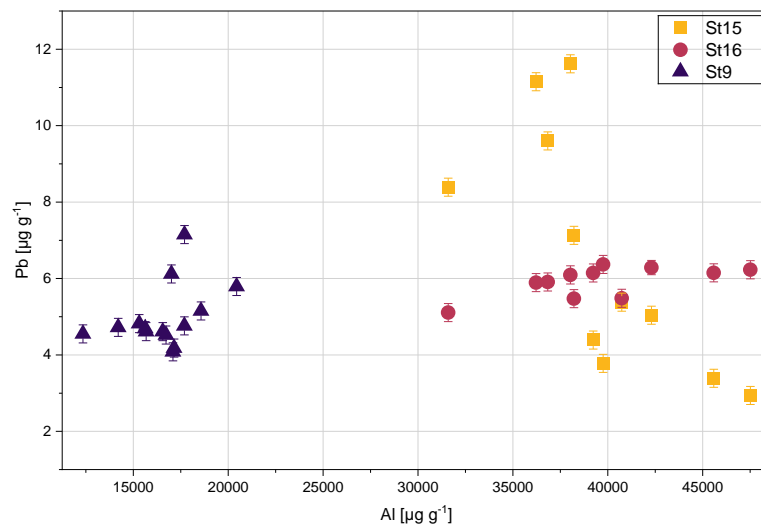


**Figure S9:** Pb concentrations plotted against Al concentrations ( $\mu\text{g g}^{-1}$ ) at all stations. Error bars are included but, in some cases, smaller than the symbols.

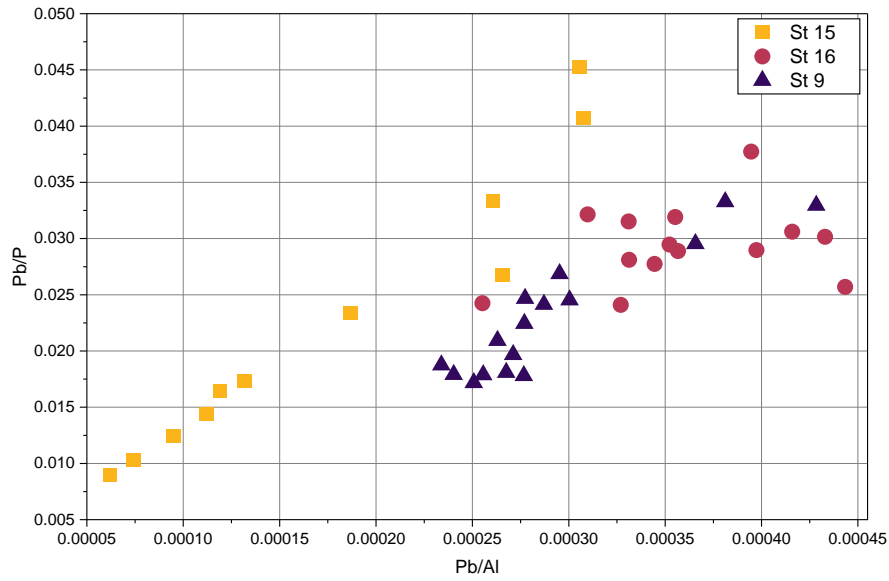


**Figure S10:** Pb/Al ratios plotted against Pb/P ratios at all stations.

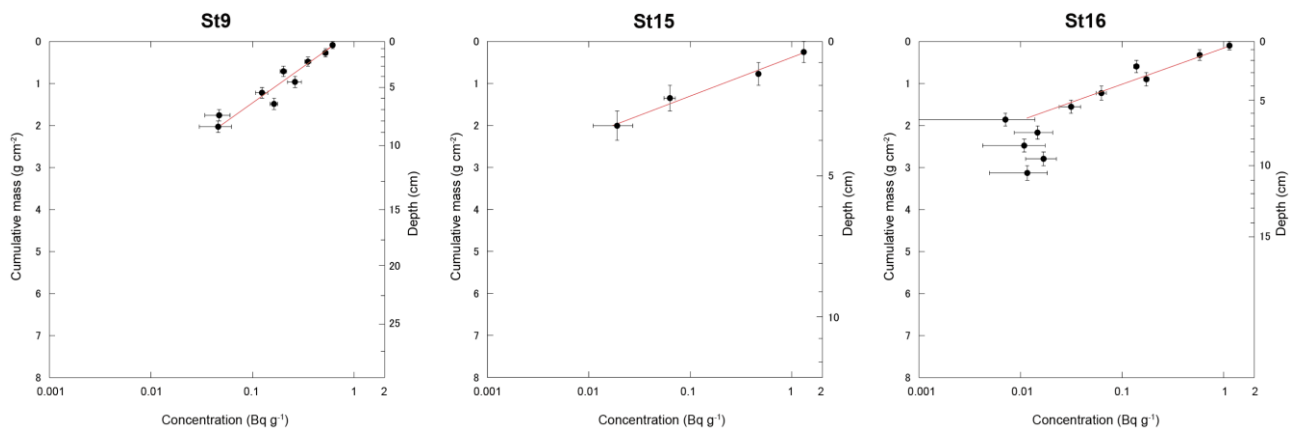


**Figure S11:** Profiles of  $^{210}\text{Pb}_{\text{ex}}$  concentrations of the sediment cores collected from St9, St15 and St16. The red exponential curves were used for deriving the mass accumulation rates.

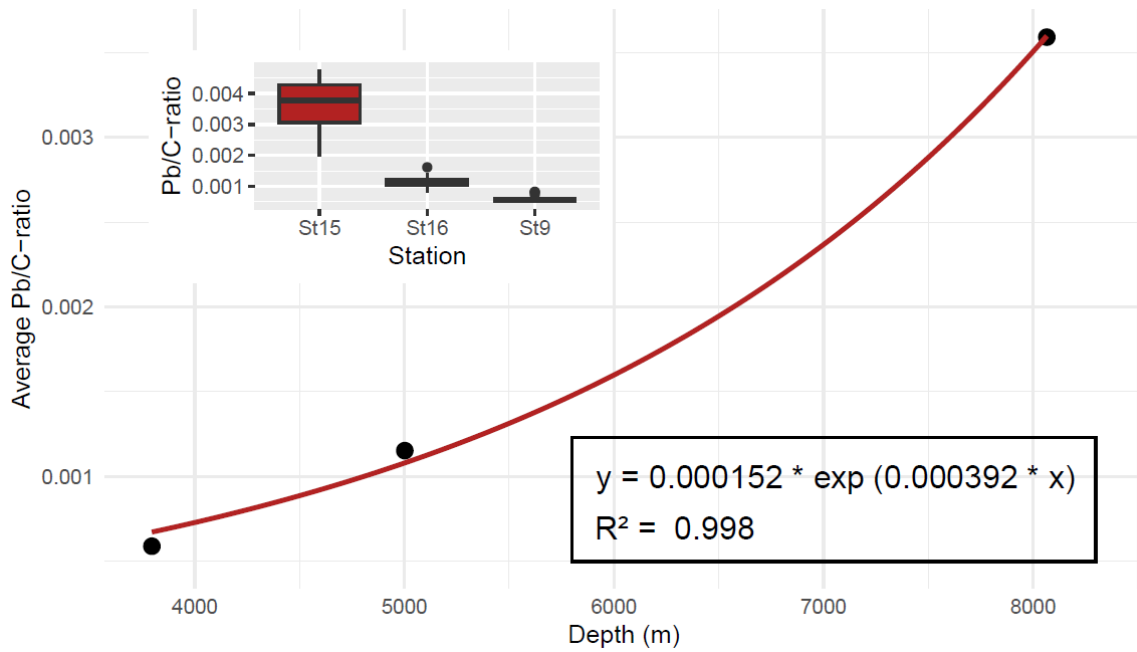


**Figure S12:** Average Pb/TOC-ratios at St9, 15 and 16 plotted against the station water depth (main panel). An exponential fit was added using the nonlinear least squares (nls) function. The inset in the upper left displays boxplots of average Pb/C-ratios at St15, 16 and 9, indicating the upper and lower quartiles, median and outliers.

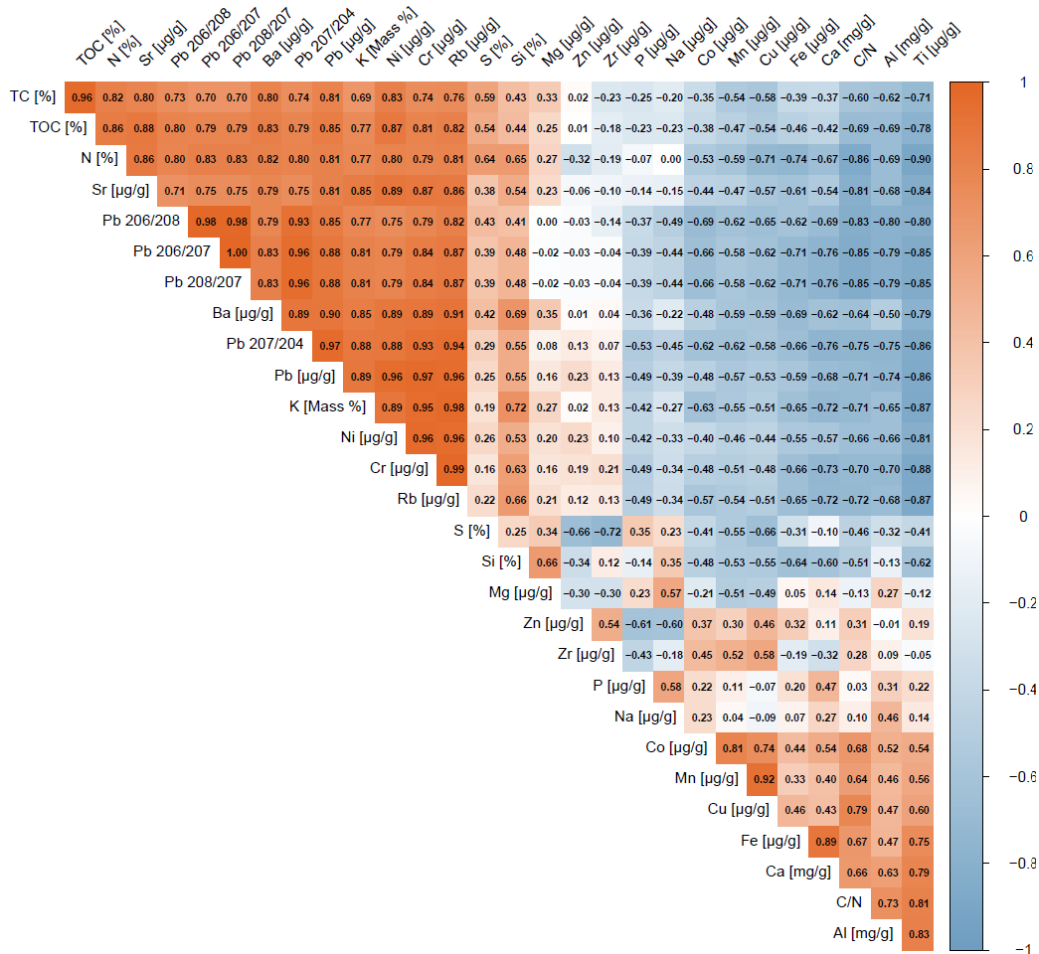


**Figure S13:** Correlation matrix for the sediments at St15. Due to the small sample size and the presence of non-normally distributed variables (Shapiro-Wilk test,  $p < 0.05$ ), Spearman rank correlation was used.

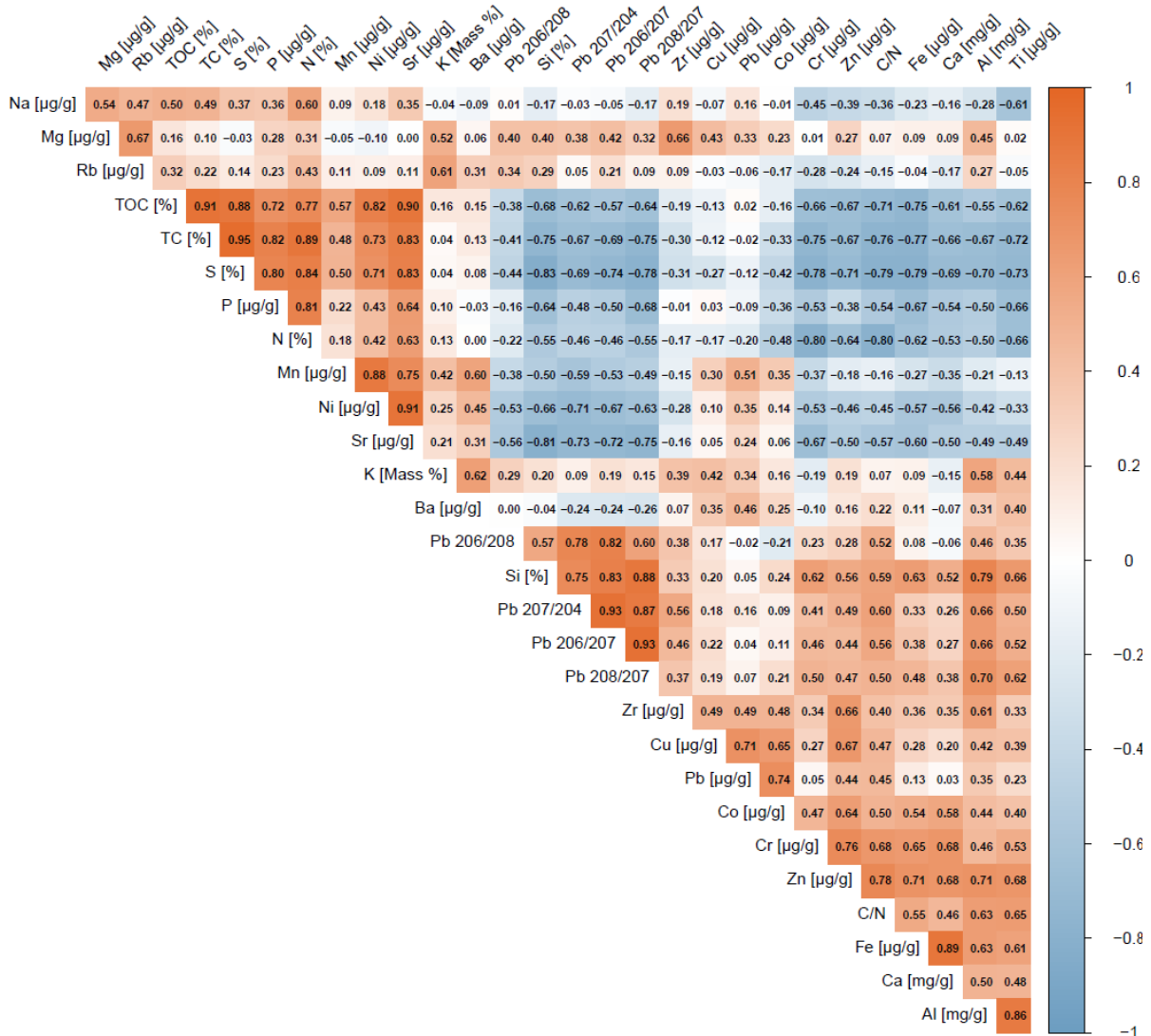


**Figure S14:** Correlation matrix for the sediments at St16. Due to the small sample size and the presence of non-normally distributed variables (Shapiro-Wilk test,  $p < 0.05$ ), Spearman rank correlation was used.

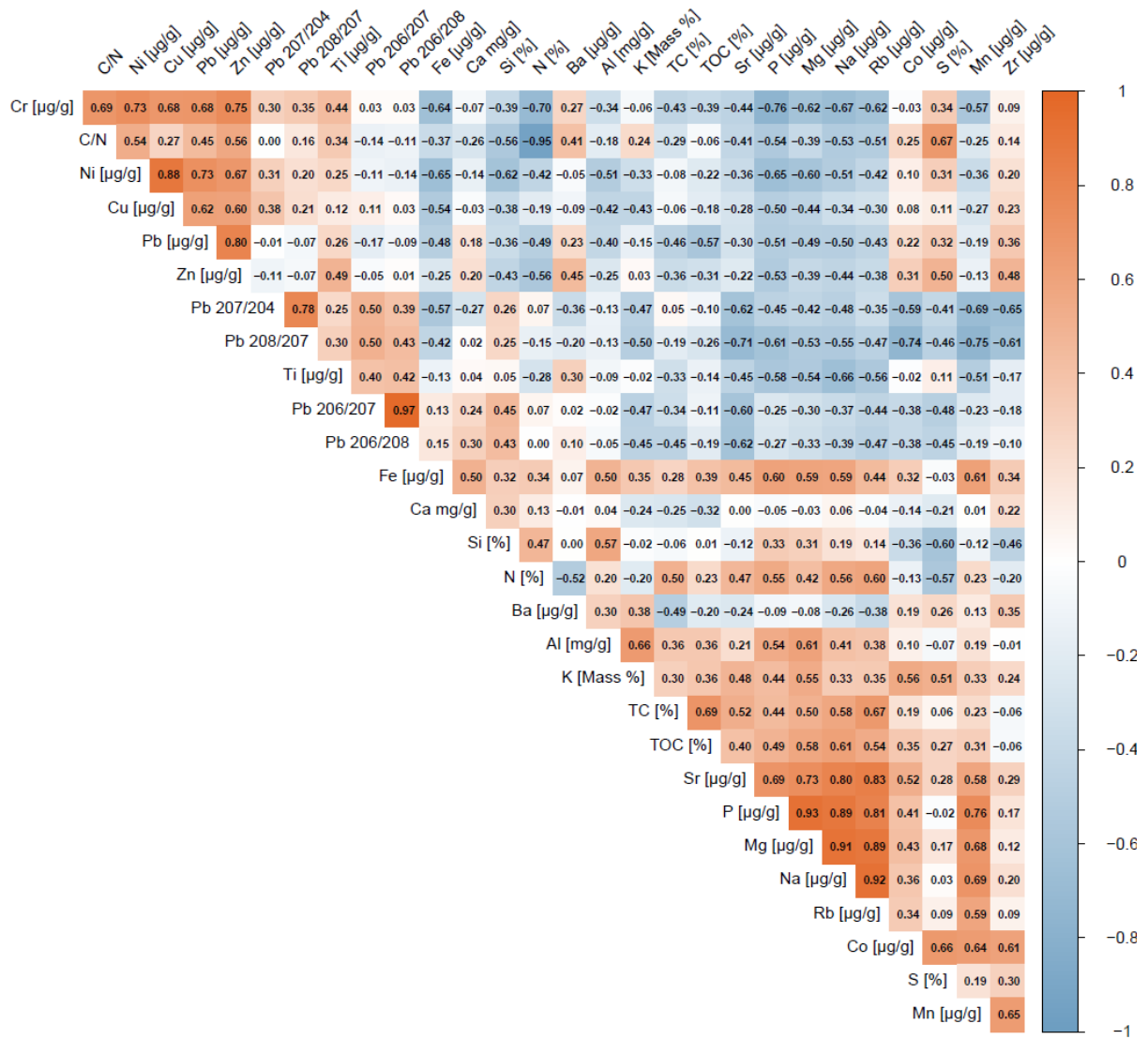


**Figure S15:** Correlation matrix for the sediments at St9. Due to the small sample size and the presence of non-normally distributed variables (Shapiro-Wilk test,  $p < 0.05$ ), Spearman rank correlation was used.

**Table S1:** Key characteristics of St9, 15 and 16.\*

	St9	St15	St16
Position	51°18'04.3"S, 39°55'31.2"W	55°13'52.3"S, 26°10'15.6"W	55°48'02.9"S, 24°50'20.6"W
Station name	South Georgia Basin	Meteor Deep, SST	Trench Margin, SST
Depth (m)	3794.8	8066.4	5002.1
Core length (cm)	26.25	12.5	13.5
Surface NPP (mg C m <sup>-2</sup> d <sup>-1</sup> )	307	195	187
O2 penetration (mm)	1.25	> 6	> 6
Chl-a (ng ml <sup>-1</sup> )	431.64	27.78	18.4
Pb conc. (µg g <sup>-1</sup> )	4.1-7.2	2.9-11.6	4.3-7.0
Pb isotope range ( <sup>206</sup> Pb/ <sup>207</sup> Pb)	1.188-1.202	1.188-1.203	1.197-1.208
Silica (%)	13.7 – 51.6	3.1-26.7	8.4-40.2
Organic carbon (%)	0.75-0.95	0.07-0.47	0.37-0.67
Sedimentation rate (mm yr <sup>-1</sup> )	0.95	0.21	0.4

\* The net primary productivity (NPP) data for the surface waters above the station sites are derived from the standard Vertically Generalized Production Model, using remote sensing data spanning from 2012 to 2021 (decadal average is provided). Overall NPP is comparably low due to significant seasonal variations at the study sites, with a high NPP during the Antarctic summer and very low NPP during the dark Antarctic winter. O2 penetration was measured in recovered sediment cores (ex situ). Chl-a data was measured in the upper 1 cm of the sediment by Astrid Bracher.

**Table S2:** Correlation coefficients of <sup>206</sup>Pb/<sup>207</sup>Pb, and <sup>208</sup>Pb/<sup>207</sup>Pb ratios and selected sediment constituents. Correlations with a *p*-value < 0.05 are considered significant.

<sup>206</sup> Pb/ <sup>207</sup> Pb vs.	Si [%]		TOC [%]		Pb [µg g <sup>-1</sup> ]		Al [mg g <sup>-1</sup> ]	
	<i>R</i>	<i>p</i>	<i>R</i>	<i>p</i>	<i>R</i>	<i>p</i>	<i>R</i>	<i>p</i>
St 15	0.4780	0.0985	0.7912	0.0012	0.8846	0.0001	-0.7912	0.0013
St16	0.8286	0.0003	-0.5736	0.0319	0.0418	0.8873	0.6571	0.0107
St9	0.4534	0.0675	-0.1127	0.6667	-0.1706	0.5128	-0.0221	0.9330
<sup>206</sup> Pb/ <sup>207</sup> Pb vs.	Mn [µg g <sup>-1</sup> ]		Fe [µg g <sup>-1</sup> ]		Ca [mg g <sup>-1</sup> ]		P [µg g <sup>-1</sup> ]	
	<i>R</i>	<i>p</i>	<i>R</i>	<i>p</i>	<i>R</i>	<i>p</i>	<i>R</i>	<i>p</i>
St 15	-0.5769	0.0390	-0.7088	0.0067	-0.7637	0.0024	-0.3867	0.1917
St16	-0.5253	0.0537	0.3758	0.1854	0.2747	0.3418	-0.5006	0.0683
St9	-0.2304	0.3737	0.1348	0.6060	0.2426	0.3480	-0.2451	0.3430
<sup>208</sup> Pb/ <sup>207</sup> Pb vs.	Si [%]		TOC [%]		Pb [µg g <sup>-1</sup> ]		Al [mg g <sup>-1</sup> ]	
	<i>R</i>	<i>p</i>	<i>R</i>	<i>p</i>	<i>R</i>	<i>p</i>	<i>R</i>	<i>p</i>
St 15	0.4780	0.0985	0.7912	0.0012	0.8846	0.0001	-0.7912	0.0013
St16	0.8813	0.0000	-0.6395	0.0137	0.0725	0.8054	0.7011	0.0052
St9	0.2525	0.3283	-0.2622	0.3092	-0.0712	0.7861	-0.1348	0.6060
<sup>208</sup> Pb/ <sup>207</sup> Pb vs.	Mn [µg g <sup>-1</sup> ]		Fe [µg g <sup>-1</sup> ]		Ca [mg g <sup>-1</sup> ]		P [µg g <sup>-1</sup> ]	
	<i>R</i>	<i>p</i>	<i>R</i>	<i>p</i>	<i>R</i>	<i>p</i>	<i>R</i>	<i>p</i>
St 15	-0.5769	0.0390	-0.7088	0.0067	-0.7637	0.0024	-0.3867	0.1917
St16	-0.4857	0.0783	0.4769	0.0846	0.3758	0.1854	-0.6792	0.0076
St9	-0.7525	0.0005	-0.4216	0.0919	0.0196	0.9405	-0.6127	0.0089

## Detailed description of the determination of Pb isotope ratios

### Sample preparation

For each digestion run, twelve sediment samples of approximately 0.15 g to 0.6 g were weighed directly into 90 mL-TFM microwave tubes (MLS GmbH, Leutkirch, Germany). Each sample was digested using 9 mL 65 % HNO<sub>3</sub> (subboiled twice, Roth ROTIPURAN® p.a., Carl Roth GmbH + Co. KG, Karlsruhe, Germany), 4 mL 48 % HF (Roth ROTIPURAN® Supra), and 3 mL 25 % HCl (subboiled twice, Bernd Kraft, AnalytiChem, Duisburg, Germany) in a ETHOS.lab microwave system (MLS GmbH, Leutkirch, Germany). Digestion was carried out within 2 h at 210 °C (25 min linear ramp from room temperature to 210°C, 50 min constant at 210 °C and 40 min cooling to room temperature). After cooling down, the solutions were evaporated to complete dryness within 4 h in a microwave heated evaporation system (MLS GmbH, Leutkirch, Germany) at 95 °C and approximately 700 mbar.

15 mL of 1 mol/L HNO<sub>3</sub> (subboiled twice, Roth ROTIPURAN® p.a.) were added to the residues. After gently shaking at room temperature for 30 s, 2 × 4 mL aliquots of the resulting clear and colorless solutions were loaded onto preconditioned 2 mL pre-packed resin columns PB-C20-A (Triskem International, Bruz, France, Lot # FPBA230215). Pb separation was carried out according to the slightly modified Eichrom application report OTS01; for details see Table S3.

**Table S3:** Pb separation sequence according to the slightly modified Eichrom application report OTS01.

Fraction	Eluent	V / mL	Aliquots	Action
1	6 mol L <sup>-1</sup> HCl	8	2 × 4 mL	Removal of Pb impurities
2	1 mol L <sup>-1</sup> HNO <sub>3</sub>	4	1 × 4 mL	Pre-conditioning
3	1 mol L <sup>-1</sup> HNO <sub>3</sub>	4	1 × 4 mL	
4	sample in 1 mol L <sup>-1</sup> HNO <sub>3</sub>	8	2 × 4 mL	Sample loading
5	1 mol L <sup>-1</sup> HNO <sub>3</sub>	16	4 × 4 mL	Matrix removal
6	6 mol L <sup>-1</sup> HCl	3	1 × 3 mL	Waste
7	6 mol L <sup>-1</sup> HCl	12	3 × 4 mL	Pb fraction
8	6 mol L <sup>-1</sup> HCl	8	2 × 4 mL	Regeneration

Each Pb fraction was collected in a 20 mL quartz tube, previously checked for Pb blanks using a QQQ-ICP-MS (Agilent 7900, Agilent Technologies Inc., Santa Clara, USA), and evaporated to dryness to remove the 6 mol L<sup>-1</sup> HCl. For this purpose, the tubes were placed in an aluminium heating block on a hot plate at 120 °C for approximately 30 h. The residues, including minor resin abrasion from the column, were redissolved in 3 mL 65 % HNO<sub>3</sub> (subboiled twice, Roth ROTIPURAN® p.a.), and evaporated to dryness within 8 h using the aluminum heating block on a hotplate at a surface temperature of up to 150 °C. In the last step, the resulting residue was redissolved in 15 mL of 1 mol L<sup>-1</sup> HNO<sub>3</sub> (subboiled twice, Roth ROTIPURAN® p.a.) to obtain a measurement solution with a Pb content of approximately  $w(\text{Pb}) \approx 100 \text{ ng g}^{-1}$ . These solutions were transferred into thoroughly pre-cleaned 15 mL PP screw-cap tubes (Sarstedt AG & Co. KG, Nümbrecht, Germany). Prior to analysis, the required aliquots were filtered through PTFE filter discs with 0.45 µm pore diameter (Chromafil Xtra GF/PTFE-45/25, Macherey-Nagel GmbH & Co. KG, Düren, Germany) using 10 mL Luer-lock PE syringes (BD DicaDit II, Becton Dickinson S.A., Fraga, Spain) directly into the pre-cleaned 4 mL PFA autosampler vials (Cetac, Omaha, USA).

All samples and the isotopic reference (prepared from NIST SRM 981) were adjusted to a Pb mass fraction of  $w(\text{Pb}) \approx 100 \text{ ng g}^{-1}$  in aqueous nitric acid with  $c(\text{HNO}_3) = 1 \text{ mol L}^{-1}$ . 20 mL PFA vials were used for the reference and the blank while 4 mL PFA vials were used for the sample solutions (Cetac, Omaha, USA).

### Pb isotop ratio measurements

Isotope ratio measurements were carried out at the Physikalisch-Technische Bundesanstalt (PTB, Braunschweig, Germany) between 7 July and 8 August 2025 using a Neptune XT multi-collector inductively coupled plasma mass spectrometer (MC-ICP-MS; Thermo Fisher Scientific, Bremen, Germany). The instrument was equipped with an ASX-110FR autosampler (Cetac, Omaha, USA), Ni skimmer and Ni sampler cones (Thermo Fisher Scientific, Bremen, Germany), an SSI Quartz dual cyclonic spray chamber (Meinhard, Golden, USA), a self-aspirating 50  $\mu\text{L}/\text{min}$  C-Flow PFA nebulizer (Saville Corporation, Eden Prairie, USA), a standard quartz torch (Thermo Fisher Scientific, Bremen, Germany), and a 1.8 mm sapphire injector (Thermo Fisher Scientific, Bremen, Germany). A class-100 laminar-flow hood (SuSi@FFU, Spetec GmbH, Erding, Germany) covering the whole sample introduction area helped to minimize contamination.

Each day, after starting the mass spectrometer, a mass calibration was performed and correct cup alignment was verified. Following a warm-up period of 1 h, the instrument was tuned for maximum sensitivity and subsequently the peak shape was checked and optimized using the focus quad. The typical sensitivity for  $^{206}\text{Pb}$  with a 100  $\text{ng g}^{-1}$  NIST SRM 981 solution was 1.65  $\text{V}/100 \text{ ng g}^{-1} = 16.5 \text{ mV}/(\text{ng g}^{-1})$  while the background signal of the 1  $\text{mol L}^{-1}$  nitric acid and the machine together were well below 0.1 mV for all isotopes at all times. The measurement sequence was started after a total warm-up period of 2 h. The cup configuration used is shown in Table S4. All Faraday cups were connected to  $10^{11} \Omega$  resistors. A gain calibration was performed once prior to the measurement campaign. The Faraday cup L3 was used to monitor possible Hg blanks in order to be able to correct the signal in L1 for  $^{204}\text{Hg}$ . Since the typical  $^{202}\text{Hg}$  signal was well below 0.05 mV in the nitric acid as well as in all references and samples, no Hg correction was applied.

**Table S4:** Cup configuration used for all measurements.

Cup	L3	L1	C	H1	H2
Isotope	$^{202}\text{Hg}$	$^{204}\text{Pb}$	$^{206}\text{Pb}$	$^{207}\text{Pb}$	$^{208}\text{Pb}$

Each measurement consisted of 20 blocks and 1 cycle/block with  $\approx 2.1 \text{ s}$  integration time and 3 s idle time. Prior to each measurement the electronic baseline was determined based on 30 cycles (1.05 s each) after a pre-baseline wait time of 10 s. During the measurements the amplifiers were not rotated. No statistical outlier rejection was applied. All raw ratios were corrected automatically for the electronic baseline and the amplifier gain. All measurements were performed in low resolution mode ( $M/\Delta M = 450$ ) with a plasma power of 1200 W. A typical sequence lasted approximately 5 h and consisted of 45 of individual measurements. Before each measurement a wash time of 90 s using 1 mol/L  $\text{HNO}_3$  (prepared from subboiled  $\text{HNO}_3$  EMSURE®, Merck KGaA, Darmstadt, Germany) and a sample take-up time of 60 s were applied. Since the 40 s baseline measurement was carried out after the take-up time was finished, the sample introduction system was rinsed with the respective sample for 100 s prior to each measurement.

At the beginning and end of each sequence, both an acid blank and a procedural blank (accounting for the full sample preparation) were measured. The procedural blank was in the lower mV range. Within each sequence, every set of four sample measurements were always bracketed between measurements of the isotopic reference. Each sequence contained additional

samples of the isotopic reference samples that underwent the complete sample preparation procedure to assess any potential effects of preparation on the measured isotope ratios. Differences between these processed and the unprocessed isotopic reference were at least one order of magnitude lower than the uncertainties meaning that the sample preparation had no significant impact on the determined isotope ratios. Therefore, no correction for sample preparation was included during the data evaluation.

The nine measurements of the isotopic references showed an average relative uncertainty of < 0.0030 % e.g. in case of  $^{206}\text{Pb}/^{208}\text{Pb}$ . The uncertainty associated with the average of the nine ratios acquired equally spaced during the 5 h sequence duration, was typically the same as the average uncertainty achieved within a single measurement (5 min duration). This indicates that no significant drift of the instrumental isotopic fraction (IIF), commonly referred to as mass bias, occurred during any sequence. Therefore, no drift correction was applied to the data. Before isotope ratio calculations, isotopic reference measurements were corrected for the acid blank, whereas processed samples were corrected for the procedural blank. Mass bias correction factors were then calculated from the blank-corrected signal intensity ratios of the isotopic reference and its certified isotope ratios, and applied to the blank-corrected sample signal intensity ratios to obtain the final sample isotope ratios.

Aliquots (i.e. subsamples from the original sediment material) of selected samples were independently processed and measured. The reproducibility of isotope ratios determined from at least three aliquots of the same samples was well within the uncertainties calculated for a single sample. Therefore, no additional uncertainty contributions accounting for the sample preparation had to be considered.

**Table S5:** MC-ICP-MS parameters applied for the measurements.

Argon	Liquid Ar 5.0, Nippon Gases Deutschland GmbH, Düsseldorf, Germany
Cool Gas	16 L/min
Aux Gas	0.80 L/min
Sample Gas	1.055 L/min
Extraction lens	-2000 V
Focus lens	-576 V
X-Deflection lens	6.25 V
Y-Deflection lens	-4.25 V
Shape lens	211 V
Rotation Quad 1	0 V
Source Offset	0 V
Focus Quad 1	-19.9 V
Rotation Quad 2	0 V
Focus Offset	50.00 V
Matsuda Plate	0 V
Zoom Optic Focus Quad	-0.50 V
Dispersion Quad	0 V

### Detailed description of the analysis of trace elements via ICP-MS / ICP-OES

Major and trace element analysis [Ca, Fe, Pb, Mn, Ni, Co, Zn, Zr, Cr]

Digestion was carried out within 2 h at 210 °C (25 min linear ramp from room temperature to 210°C, 50 min constant at 210 °C and 40 min cooling to room temperature). The solutions were evaporated to complete dryness within 4 h in a microwave heated evaporation system (MLS GmbH, Leutkirch, Germany) at 95 °C and approximately 700 mbar.

Trace element analysis [Pb, Mn, Ni, Co, Zn, Zr, Cr], was conducted in two separated runs using an 8900 ICP-MS Triple Quadrupole by Agilent Technologies. To remain within the limits of quantification of both calibration curve and measuring device, the digested samples were diluted by a factor of 10 and 25. Limits of detection (LOD) and limits of quantification (LOQ) were determined according to DIN 32645 via blank-measurements (0) and the calibration curve (Cal) using the following equations.

Determination of the LOD:

$$x_{LOD} = \frac{s_y}{m} * t * \sqrt{\frac{1}{\hat{N}} + \frac{1}{N}} \quad (1)$$

$m$  = Slope of the calibration curve

$s_y$  = Standard deviation of blank values

$t$  =  $t$ -value extracted from table;  $f = N - 1$ ;  $P = 95\%$ )

$\hat{N}$  = Number of parallel measurements

$N$  = Number of blank values

Determination of the LOQ:

$$x_{LOQ} = k * s_{x0} * t * \sqrt{\frac{1}{\hat{N}} + \frac{1}{N} + \frac{(k * x_{NG} - \bar{x})^2}{Q_x}} \quad (2)$$

$k$  = Factor, 3 is recommended (corresponds to 33.33% uncertainty)

$s_{x0}$  = Process standard deviation of the calibration curve

$t$  =  $t$ -value extracted from table;  $f = N - 2$ ;  $P = 95\%$ )

$\hat{N}$  = Number of parallel measurements

$N$  = Number of blank values

$\bar{x}$  = Arithmetic means of the concentrations of all calibration samples

$x_{NG}$  = Limit of detection

$Q_x = \Sigma(x_i - \bar{x})^2$

$x_i$  = Individual concentrations of all calibration samples

All measured concentrations were corrected by subtracting the blank values and exclusion of those with concentrations below the LOQ.

**Table S6:** Certified values for reference material IAEA 456 ( $n = 12$ ) and measured average concentrations and standard deviations (SD) of the digested material.

Element	Cr ( $\mu\text{g L}^{-1}$ )	Mn ( $\mu\text{g L}^{-1}$ )	Ni ( $\mu\text{g L}^{-1}$ )	Cu ( $\mu\text{g L}^{-1}$ )	Zr ( $\mu\text{g L}^{-1}$ )	Pb ( $\mu\text{g L}^{-1}$ )	Fe ( $\mu\text{g L}^{-1}$ )
Certified value	589	825	760	44.6	-	33.4	49500
Expanded uncertainty	42	52	56	2.4	-	2.1	3200
Average conc.	479.24	711.67	738.49	39.02	54.47	33.68	44776.6
SD conc.	68.62	128.75	106.23	4.66	11.62	3.55	4174.6

Iron (Fe) and calcium (Ca) concentrations in the digested samples were determined using an inductively couple plasma – optic emission spectrometry (ICP-OES) ES 715 by Varian (now

Agilent Technologies). A calibration was performed previous to each measurement using a calibration standard in different increments from 0.5 to 100 %. To stay within the concentration limits of calibration curve and measuring device, digested samples were diluted by a factor of 10, 50 or 100 prior to measuring.

### CNS analysis

Total Carbon (TC), Nitrogen (N) and Sulfur (S) concentrations in the solid samples were determined using an Element-analyzer Euro EA 3000 by HEKAtec at TU Braunschweig. Calibration was performed using certified BBOT and sulfanilamide standards. Samples weighing between 4 - 6 mg were placed into tin cartridges; with a small amount of vanadium pentoxide added to each cartridge to ensure a complete ignition. For total organic carbon (TOC) analyses, inorganic carbonates were removed by pre-treating the samples with 2 molar hydrochloric acid as follows: 10 mg of the sediment were weighed into silver cartridges, 50  $\mu$ L of hydrochloric acid were added and the cartridges were placed on heating plates at 75 °C for 60 minutes or until dryness. The process was repeated until no reaction was observed, usually until ca. 150 – 200  $\mu$ L of HCl was used. After that the cartridges were left on the heating plate overnight so they could fully dry. Then, vanadium pentoxide was added to the samples, the silver cartridges were closed and placed in tin cartridges for better ignition and measured in the Element-analyzer as described for TC. Reference materials and sulfanilamide standards were measured regularly for quality control, the results of which are given in Table S7. Triple measurements were conducted in regular intervals of eight samples.

**Table S7:** Certified TOC contents for reference materials and measured average concentrations and standard deviations (SD). The number of repeated measurements are indicated by *n*.

Parameter	Reference Material	<i>n</i>	Certified values	Average	SD
TOC	China Sediment NCS DC 73019	3	0.32 +/- 0.04	0.36	0.02
TOC	China Sediment 73048	2	0.17 (recommended)	0.242	0.008
TC	China Sediment NCS DC 73019	3	1.46 +/-0.08	1.56	0.02
TC	China Sediment 73048	3	0.21 (recommended)	0.233	0.011

## <sup>210</sup>Pb Dating of sediment cores

All data regarding <sup>210</sup>Pb<sub>ex</sub> concentrations is provided in Table S8.

**Table S8:** Depth, Cumulative mass, and <sup>210</sup>Pb<sub>ex</sub> concentrations of St9, St15, and S516 cores.

<b>St9</b>					
Depth	Range ±	Cumulative mass	Range ±	<sup>210</sup> Pb <sub>ex</sub>	Error
(cm)	(cm)	(g cm <sup>-2</sup> )	(g cm <sup>-2</sup> )	(Bq g <sup>-1</sup> )	(Bq g <sup>-1</sup> )
0.5	0.5	0.085	0.085	0.615	0.031
1.5	0.5	0.271	0.100	0.523	0.031
2.5	0.5	0.480	0.109	0.352	0.024
3.5	0.5	0.710	0.121	0.202	0.015
4.5	0.5	0.962	0.131	0.262	0.041
5.5	0.5	1.221	0.128	0.124	0.017
6.5	0.5	1.485	0.135	0.163	0.014
7.5	0.5	1.756	0.136	0.047	0.013
8.5	0.5	2.029	0.138	0.046	0.016
9.5	0.5	2.323	0.156		
11.25	1.25	2.906	0.428		
13.75	1.25	3.666	0.333		
16.25	1.25	4.361	0.362		
18.75	1.25	5.027	0.304		
21.25	1.25	5.689	0.359		
23.75	1.25	6.387	0.340		
26.25	1.25	7.048	0.321		
<b>St15</b>					
Depth	Range ±	Cumulative mass	Range ±	<sup>210</sup> Pb <sub>ex</sub>	Error
(cm)	(cm)	(g cm <sup>-2</sup> )	(g cm <sup>-2</sup> )	(Bq g <sup>-1</sup> )	(Bq g <sup>-1</sup> )
0.5	0.5	0.251	0.251	1.313	0.032
1.5	0.5	0.773	0.272	0.469	0.019
2.5	0.5	1.351	0.306	0.063	0.008
3.5	0.5	2.006	0.349	0.019	0.008
4.5	0.5	2.779	0.424		
5.5	0.5	3.569	0.367		
6.5	0.5	4.280	0.344		
7.5	0.5	4.953	0.329		
8.5	0.5	5.621	0.340		
9.5	0.5	6.260	0.299		
10.5	0.5	6.816	0.257		
11.5	0.5	7.355	0.281		
12.5	0.5	7.948	0.312		

<b>St16</b>					
Depth	Range $\pm$	Cumulative mass	Range $\pm$	$^{210}\text{Pb}_{\text{ex}}$	Error
(cm)	(cm)	(g cm <sup>-2</sup> )	(g cm <sup>-2</sup> )	(Bq g <sup>-1</sup> )	(Bq g <sup>-1</sup> )
0.5	0.5	0.098	0.098	1.141	0.018
1.5	0.5	0.322	0.126	0.581	0.014
2.5	0.5	0.594	0.146	0.138	0.008
3.5	0.5	0.900	0.159	0.173	0.010
4.5	0.5	1.229	0.170	0.063	0.007
5.5	0.5	1.554	0.154	0.032	0.008
6.5	0.5	1.860	0.152	0.007	0.007
7.5	0.5	2.170	0.157	0.015	0.006
8.5	0.5	2.478	0.151	0.011	0.007
9.5	0.5	2.793	0.164	0.017	0.006
10.5	0.5	3.130	0.173	0.012	0.007
11.5	0.5	3.464	0.161		
12.5	0.5	3.798	0.173		
13.5	0.5	4.145	0.174		
14.5	0.5	4.486	0.166		